Calculation of a strongly swirling turbulent round jet with recirculation by an algebraic stress model

Kwang Yong Kim* and Myung Kyoon Chung
Department of Mechanical Engineering,
Korea Advanced Institute of Science and Technology, Cheongryang, Seoul, Korea

Received 5 January 1987; accepted 11 June 1987

The algebraic stress model is applied to a turbulent swirling round jet with recirculation, and the prediction is compared with that of the standard k-ε model and experimental data. The anisotropic eddy viscosities in three directions are assumed in a way similar to the Boussinesq eddy viscosity hypothesis as functions of the mean velocity gradients, the turbulent kinetic energy, and its dissipation rate. The results show that the algebraic stress model yields very good agreement with experimental data on both axial and tangential velocity distributions.

Keywords: algebraic stress model; turbulence; swirl; jet; recirculation; eddy viscosity

Introduction

Turbulent swirling flow has important engineering applications in gas turbine combustors and furnaces. A strong swirl with a swirl number larger than 0.5 imparted onto a round jet produces a recirculation zone around the jet axis near the nozzle exit, which provides efficient mixing of the fuel with the surrounding air and the combustion products.

Many experimental investigators[1-6] have offered measurements of mean and turbulent quantities in the swirling jet, which have been extensively reviewed by Morse.[7] In particular, in the case with recirculation, Sislian and Cusworth[6] provided LDV measurements of the profiles of three mean velocity components and all six Reynolds stress components at the nozzle exit and the downstream locations.

The swirl imparted to the turbulent flow significantly modifies the turbulent structure, as described in the above experimental investigations, and thus any computational turbulence model for swirling flows must take the swirl effect on turbulence into account. The existence of recirculation is also an important factor for development of the turbulence model. The conventional turbulence models, such as the mixing length model and the two-equation models, originally proposed for simple shear layers must thus be modified to take into account the effect of swirl. For this purpose, Bradshaw[8] proposed a simple empirical correction for mixing length, based on the analogy between streamline curvature and buoyancy. Similar approaches to the length scale of the k-ε model were also used, by Launder, Priddin, and Sharma[9] and Rodi,[10] but they showed limited applicability, as proved by Leschziner and Rodi[11] and Chen.[12] Leschziner and Rodi[11] reported their computational results of a strongly swirling jet and concluded that the standard k-ε model gives results better than those of any swirl-corrected k-ε model in the case with recirculation.

The Reynolds stress transport model as a second-order closure scheme is regarded as a most logical approach to the turbulence closure problem, which does not need any ad hoc modification for extra strain rates. However, for the prediction of swirling flow with recirculation, it is necessary to solve a total of 11 governing differential equations of elliptic type: a continuity equation, three momentum equations, an ε-equation, and six equations for the Reynolds stresses. Thus, the computational complexity with this model is considerable. For the swirling flows without recirculation, there have been a few numerical investigations with the Reynolds stress model, such as those by Launder and Morse,[13] Higuchi and Rubesin,[14] Ettestad and Lumley,[15] and Gibson and Younis.[16,17] Gibson and Younis[16] presented computations of weakly swirling jets of which agreements with experiments are satisfactory.

Compared with the Reynolds stress model, the algebraic stress model, which has been successfully used for other types of complex turbulent flows,[18] should be an economic yet reasonably accurate computational method if the swirl effect is reflected in the governing equations in an appropriate way. There can be several other types of algebraic stress model, depending on the approximation and the way in which k and ε are obtained. Koosinlin and Lockwood[19] applied their algebraic stress model to the calculation of boundary layer flows over rotating bodies. They obtained k and ε from equations for k and the turbulent length scale. For the prediction of diffuser flows with inlet swirl, Hah[20] used the algebraic stress model with the k and ε equations, which introduces the approximation other than that of Koosinlin and Lockwood[19] for the collective effect of convection and diffusion terms in the stress equation.

The present work investigates another type of algebraic stress model for the calculation of swirling flow with recirculation. For weakly swirling flows without recirculation, a new, simple correction method for the k-ε model, which takes into account the effect of swirl, has been derived from this algebraic stress model in a previous work.[21]

The main purpose of the present work is to show that the effects of swirl and recirculation in a strongly swirling round jet can be correctly reproduced by the algebraic stress model. For this purpose, the experiment of Sislian and Cusworth[6] is selected as a test flow.

Turbulence model

The equation for the Reynolds stress tensor represented by Launder, Reece, and Rodi[22] is

$$\frac{D\overline{u_i u_j}}{Dt} = D_{ij} + P_{ij} + \phi_{ij} - \tfrac{2}{3}\delta_{ij}\varepsilon \qquad (1)$$

* Present address: Department of Mechanical Engineering, Inha University, Inchon, Korea

where

$$D_{ij}=c_s\frac{\partial}{\partial x_k}\left(\frac{k}{\varepsilon}\overline{u_k u_l}\,\frac{\partial\overline{u_i u_j}}{\partial x_l}\right) \tag{2}$$

$$P_{ij}=-\overline{u_i u_k}\,\frac{\partial U_j}{\partial x_k}-\overline{u_j u_k}\,\frac{\partial U_i}{\partial x_k} \tag{3}$$

$$\phi_{ij}=-c_1\frac{\varepsilon}{k}\left(\overline{u_i u_j}-\tfrac{2}{3}\delta_{ij}k\right)-c_2\left(P_{ij}-\tfrac{2}{3}\delta_{ij}P\right) \tag{4}$$

indicate the diffusion, production, and pressure strain tensors, respectively. Here, the production rate of k is defined by $P=-\overline{u_k u_l}(\partial U_k/\partial x_l)$. The derivation of the algebraic stress equation starts from Equation 1. According to Ref. 23, the assumption of constant $\overline{u_i u_j}/k$ allows the following simplification:

$$\frac{D\overline{u_i u_j}}{Dt}-D_{ij}=\frac{\overline{u_i u_j}}{k}(P-\varepsilon) \tag{5}$$

Substitution of Equation 5 into Equation 1 converts the differential equation 1 to an algebraic equation, which after some manipulations, reduces to

$$\frac{\overline{u_i u_j}}{k}=\phi_1\frac{P_{ij}}{\varepsilon}+\phi_2\delta_{ij} \tag{6}$$

where

$$\phi_1=\frac{1-c_2}{P/\varepsilon+c_1-1}\qquad\text{and}\qquad\phi_2=\frac{2}{3}\frac{c_2P/\varepsilon+c_1-1}{P/\varepsilon+c_1-1}$$

The model constants are taken as $c_1=1.8$ and $c_2=0.6$ in this work; these have been used by Gibson[24] in the calculation of shear flow with streamline curvature.

For the axisymmetric swirling flows, each production tensor is expressed in cylindrical coordinates as follows:

$$P_{11}=-\left(2\overline{u^2}\,\frac{\partial U}{\partial x}+2\overline{uv}\,\frac{\partial U}{\partial r}\right) \tag{7}$$

$$P_{22}=-\left(2\overline{uv}\,\frac{\partial V}{\partial x}+2\overline{v^2}\,\frac{\partial V}{\partial r}-2\frac{W}{r}\overline{vw}\right) \tag{8}$$

$$P_{33}=-\left(2\overline{uw}\,\frac{\partial W}{\partial x}+2\overline{vw}\,\frac{\partial W}{\partial r}+2\frac{V}{r}\overline{w^2}\right) \tag{9}$$

$$P_{12}=-\left(\overline{uv}\,\frac{\partial U}{\partial x}+\overline{v^2}\,\frac{\partial U}{\partial r}+\overline{u^2}\,\frac{\partial V}{\partial x}+\overline{uv}\,\frac{\partial V}{\partial r}-\frac{W}{r}\overline{uw}\right) \tag{10}$$

$$P_{13}=-\left(\overline{uw}\,\frac{\partial U}{\partial x}+\overline{vw}\,\frac{\partial U}{\partial r}+\overline{u^2}\,\frac{\partial W}{\partial x}+\overline{uv}\,\frac{\partial W}{\partial r}+\frac{V}{r}\overline{uw}\right) \tag{11}$$

$$P_{23}=-\left(\overline{uw}\,\frac{\partial V}{\partial x}+\overline{vw}\,\frac{\partial V}{\partial r}+\overline{uv}\,\frac{\partial W}{\partial x}+\overline{v^2}\,\frac{\partial W}{\partial r}+\frac{V}{r}\overline{vw}-\frac{W}{r}\overline{w^2}\right) \tag{12}$$

where the subscripts 1, 2, and 3 indicate x, r, and θ coordinates, respectively. From Equations 7–9, expressions for normal stress components are derived from Equation 6 in terms of shear stresses.

$$\overline{u^2}=-C_u\left(2\overline{uv}\,\frac{\partial U}{\partial r}-\frac{\phi_2}{\phi_1}\varepsilon\right) \tag{13}$$

$$\overline{v^2}=-C_v\left(-2\frac{W}{r}\overline{vw}+2\overline{uv}\,\frac{\partial V}{\partial x}-\frac{\phi_2}{\phi_1}\varepsilon\right) \tag{14}$$

$$\overline{w^2}=-C_w\left(2\overline{uw}\,\frac{\partial W}{\partial x}+2\overline{vw}\,\frac{\partial W}{\partial r}-\frac{\phi_2}{\phi_1}\varepsilon\right) \tag{15}$$

where

$$C_u=\frac{\phi_1 k/\varepsilon}{1+2\phi_1(k/\varepsilon)(\partial U/\partial x)},\qquad C_v=\frac{\phi_1 k/\varepsilon}{1+2\phi_1(k/\varepsilon)(\partial V/\partial r)},$$

and

$$C_w=\frac{\phi_1 k/\varepsilon}{1+2\phi_1 kV/\varepsilon r}$$

Then Equation 6 and Equations 10–15 yield the following equations for the shear stresses:

$$-\overline{uv}=\frac{\phi_1\frac{k}{\varepsilon}\left(2C_v\overline{vw}\,\frac{W}{r}\frac{\partial U}{\partial r}-\overline{uw}\,\frac{W}{r}\right)+\phi_2 k\left(C_u\frac{\partial V}{\partial x}+C_v\frac{\partial U}{\partial r}\right)}{1+\phi_1\frac{k}{\varepsilon}\left(\frac{\partial U}{\partial x}+\frac{\partial V}{\partial r}\right)-2\phi_1(C_u+C_v)\frac{k}{\varepsilon}\frac{\partial U}{\partial r}\frac{\partial V}{\partial x}} \tag{16}$$

$$-\overline{vw}=\frac{\phi_1\frac{k}{\varepsilon}\left(\overline{uv}\,\frac{\partial W}{\partial x}+\overline{uw}\,\frac{\partial V}{\partial x}-2C_v\overline{uv}\,\frac{\partial V}{\partial x}\frac{\partial W}{\partial r}+2C_w\overline{uw}\,\frac{W}{r}\frac{\partial W}{\partial x}\right)+\phi_2 k\left(C_v\frac{\partial W}{\partial r}-C_w\frac{W}{r}\right)}{1+\phi_1\frac{k}{\varepsilon}\left(\frac{\partial V}{\partial r}+\frac{V}{r}\right)+2\phi_1(C_v+C_w)\frac{k}{\varepsilon}\frac{W}{r}\frac{\partial W}{\partial r}} \tag{17}$$

$$-\overline{uw}=\frac{\phi_1\frac{k}{\varepsilon}\left(\overline{vw}\,\frac{\partial U}{\partial r}+\overline{uv}\,\frac{\partial W}{\partial r}-2C_u\overline{uv}\,\frac{\partial U}{\partial r}\frac{\partial W}{\partial x}\right)+\phi_2 kC_u\frac{\partial W}{\partial x}}{1+\phi_1\frac{k}{\varepsilon}\left(\frac{\partial U}{\partial x}+\frac{V}{r}\right)} \tag{18}$$

Notation

c_1, c_2, c_s	Turbulence model constants
C_u, C_v, C_w	Parameters in Equations 13–15, respectively
D	Diameter of nozzle exit
D_{ij}	Rate of diffusion of $\overline{u_i u_j}$, Equation 2
k	Turbulent kinetic energy
N_r, N_x	Numbers of grid points in radial and axial directions, respectively
P	Rate of production of k
P_{ij}	Rate of production tensor of $\overline{u_i u_j}$, Equation 3
$\bar{P}$	Pressure
r	Radial coordinate
S_x, S_r, S_θ	Parameters in Equations 23–25, respectively
U, V, W	Axial, radial, and tangential mean velocity components, respectively
$\rho\overline{u_i u_j}$	Reynolds stress tensor
$\rho\overline{uv}, \rho\overline{vw}, \rho\overline{uw}$	Reynolds shear stresses
$\rho\overline{u^2}, \rho\overline{v^2}, \rho\overline{w^2}$	Reynolds normal stresses
x	Axial coordinate
δ_{ij}	Kronecker delta
ε	Rate of dissipation of k
θ	Tangential coordinate
ν_t	Eddy viscosity defined by Equation 28
$\nu_{t_1}, \nu_{t_2}, \nu_{t_3}$	Eddy viscosities defined by Equations 19–21, respectively
ρ	Density
ϕ_1, ϕ_2	Parameters in Equation 6
ϕ_{ij}	Pressure-strain correlation term, Equation 4

Further manipulation makes it possible to express each shear stress component in the form which does not include any other stress component. Thus, all six stress components can be determined from the solutions of k, ε, and the mean flow equations.

For convenience, the following expressions for eddy viscosities are introduced as in Ref. 25:

$$\nu_{t_1}=\frac{-\overline{uv}}{\partial V/\partial x+\partial U/\partial r} \tag{19}$$

$$\nu_{t_2}=\frac{-\overline{vw}}{\partial W/\partial r-W/r} \tag{20}$$

$$\nu_{t_3}=\frac{-\overline{uw}}{\partial W/\partial x} \tag{21}$$

Actually, these definitions of the eddy viscosities represent the strong dependence of shear stresses on the local strain rates of the mean flow, which has been found in the experiment of the swirling jet with recirculation by Sislian and Cusworth.[6] Equations 19–21 also imply the anisotropy of turbulent eddy viscosities which the standard k-ε model does not take into account. Then the mean flow equations for axisymmetric swirling flow take the following forms:

Continuity equation

$$\frac{\partial U}{\partial x}+\frac{1}{r}\frac{\partial(rV)}{\partial r}=0 \tag{22}$$

Momentum equations

$$U\frac{\partial U}{\partial x}+V\frac{\partial U}{\partial r}=-\frac{1}{\rho}\frac{\partial \bar{P}}{\partial x}+\frac{1}{r}\frac{\partial}{\partial r}\left(\nu_{t_1}r\frac{\partial U}{\partial r}\right)+\frac{\partial}{\partial x}\left(\nu_{t_1}\frac{\partial U}{\partial x}\right)+S_x \tag{23}$$

$$U\frac{\partial V}{\partial x}+V\frac{\partial V}{\partial r}-\frac{W^2}{r}=-\frac{1}{\rho}\frac{\partial \bar{P}}{\partial r}+\frac{1}{r}\frac{\partial}{\partial r}\left(\nu_{t_1}r\frac{\partial V}{\partial r}\right)+\frac{\partial}{\partial x}\left(\nu_{t_1}\frac{\partial V}{\partial x}\right)+S_r \tag{24}$$

$$U\frac{\partial W}{\partial x}+V\frac{\partial W}{\partial r}+\frac{VW}{r}=\frac{1}{r}\frac{\partial}{\partial r}\left(\nu_{t_2}r\frac{\partial W}{\partial r}\right)+\frac{\partial}{\partial x}\left(\nu_{t_3}\frac{\partial W}{\partial x}\right)+S_\theta \tag{25}$$

where

$$S_x=\frac{1}{r}\frac{\partial}{\partial r}\left(\nu_{t_1}r\frac{\partial V}{\partial x}\right)+\frac{\partial}{\partial x}\left(\nu_{t_1}\frac{\partial U}{\partial x}\right)$$

$$S_r=\frac{1}{r}\frac{\partial}{\partial r}\left(\nu_{t_1}r\frac{\partial V}{\partial r}\right)+\frac{\partial}{\partial x}\left(\nu_{t_1}\frac{\partial U}{\partial r}\right)-2\nu_{t_1}\frac{V}{r^2}$$

$$S_\theta=-\frac{\partial}{\partial r}\left(\nu_{t_2}\frac{W}{r}\right)+\frac{\nu_{t_2}}{r}\frac{\partial W}{\partial r}-2\nu_{t_2}\frac{W}{r^2}$$

The above algebraic stress model uses the following equations for k and ε:

$$U\frac{\partial k}{\partial x}+V\frac{\partial k}{\partial r}=\frac{\partial}{\partial x}\left(\frac{\nu_t}{\sigma_k}\frac{\partial k}{\partial x}\right)+\frac{1}{r}\frac{\partial}{\partial r}\left(r\frac{\nu_t}{\sigma_k}\frac{\partial k}{\partial r}\right)+P-\varepsilon \tag{26}$$

$$U\frac{\partial \varepsilon}{\partial x}+V\frac{\partial \varepsilon}{\partial r}=\frac{\partial}{\partial x}\left(\frac{\nu_t}{\sigma_\varepsilon}\frac{\partial \varepsilon}{\partial x}\right)+\frac{1}{r}\frac{\partial}{\partial r}\left(r\frac{\nu_t}{\sigma_\varepsilon}\frac{\partial \varepsilon}{\partial r}\right)+C_{\varepsilon 1}\frac{\varepsilon}{k}P-C_{\varepsilon 2}\frac{\varepsilon^2}{k} \tag{27}$$

where

$$\nu_t=C_\mu\frac{k^2}{\varepsilon} \tag{28}$$

The model constants are $\sigma_k=1.$, $\sigma_\varepsilon=1.22$, $C_{\varepsilon 1}=1.44$, $C_{\varepsilon 2}=1.92$, and $C_\mu=0.09$, which have been suggested in Ref. 26.

When the eddy viscosities ν_{t_1}, ν_{t_2}, and ν_{t_3} are replaced by ν_t, Equations 22–27 are reduced to the equations of the standard k-ε model.

Computational results and discussions

The boundary conditions used here are summarized in Table 1, and the calculation domain is shown in Figure 1. The computational inlet plane was located at $x/D=0.125$, where experimental data are available. The inlet conditions for velocity components and k have been obtained from the experiment, and the dissipation rate, which is not available from experiment directly, is calculated by the equation shown in Table 1, using the experimental data of $\overline{uv}$.

The computer program was based on a modified version of

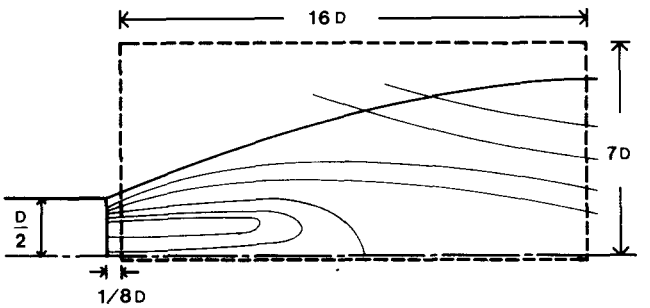

Figure 1 Calculation domain

Table 1 Boundary condition

Boundary \ Variable	U	V	W	k	ε
Inlet	Experimental data	Experimental data	Experimental data	Experimental data	$\varepsilon=0.09\frac{k^2}{\overline{uv}}\frac{\partial U}{\partial r}$
Symmetric axis	$\frac{\partial U}{\partial r}=0$	0	0	$\frac{\partial k}{\partial r}=0$	$\frac{\partial \varepsilon}{\partial r}=0$
Outlet	$\frac{\partial^2 U}{\partial x^2}=0$	A	$\frac{\partial^2 W}{\partial x^2}=0$	$\frac{\partial k}{\partial x}=0$	$\frac{\partial \varepsilon}{\partial x}=0$
Entrainment boundary	0	B	0	0	0

A: V computed from continuity equation.
B: V computed from r-momentum equation with $rV\equiv$constant.

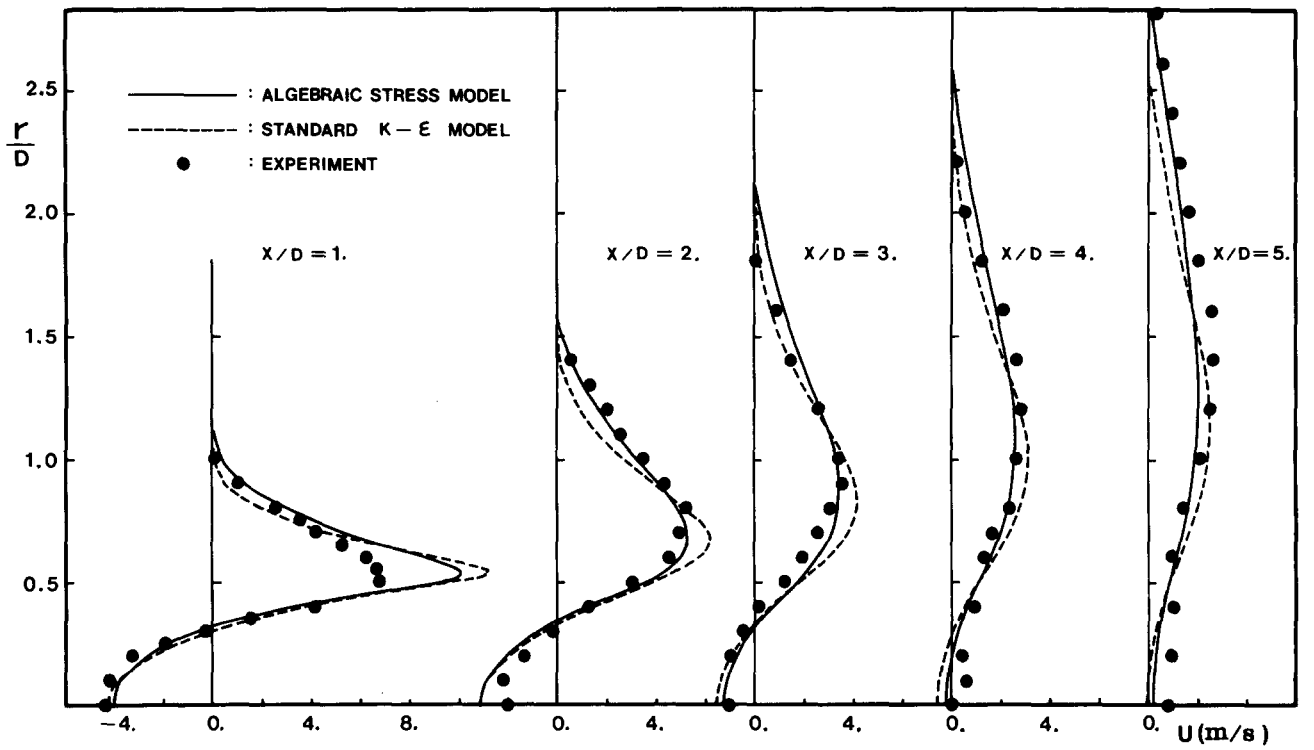

Figure 2 Distributions of axial velocity

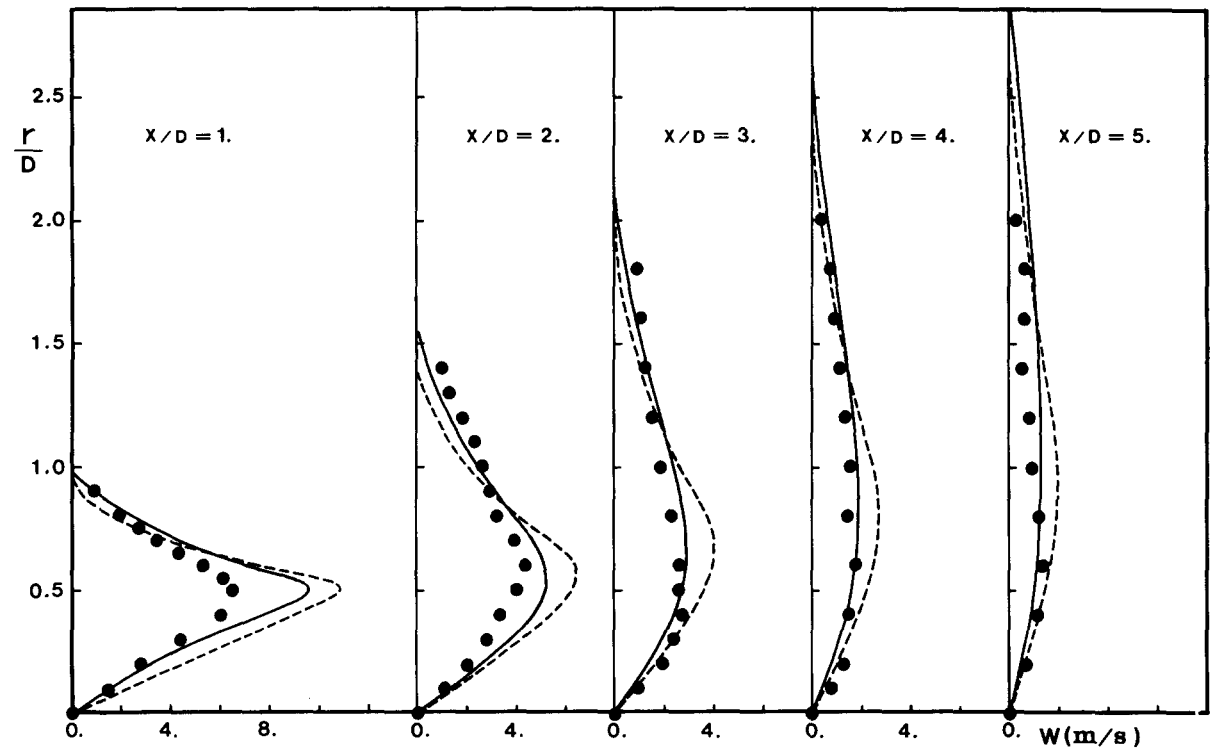

Figure 3 Distributions of tangential velocity (symbols as in Figure 2)

TEACH.[26] Convection terms in the governing equations were discretized by the hybrid central/upwind difference scheme. The computational mesh consisted of 37×24 ($N_r \times N_x$) nonuniformly distributed nodes. Twenty-four nodes in the r-direction and eight nodes in the x-direction are concentrated in $r/D < 1$ and $x/D < 2$, respectively. The grid dependence test with the k-ε model showed that the finer mesh scheme (47×28) yields a length of recirculation only 2% larger than the present mesh scheme. The converged solutions were obtained after more than 1000 iterations. The underrelaxation factors were 0.5 for the mean velocity components and 0.7 for k, ε, and eddy viscosity with the k-ε model, and were 0.2 and 0.1, respectively, with the algebraic stress model.

The computations have been performed with an algebraic

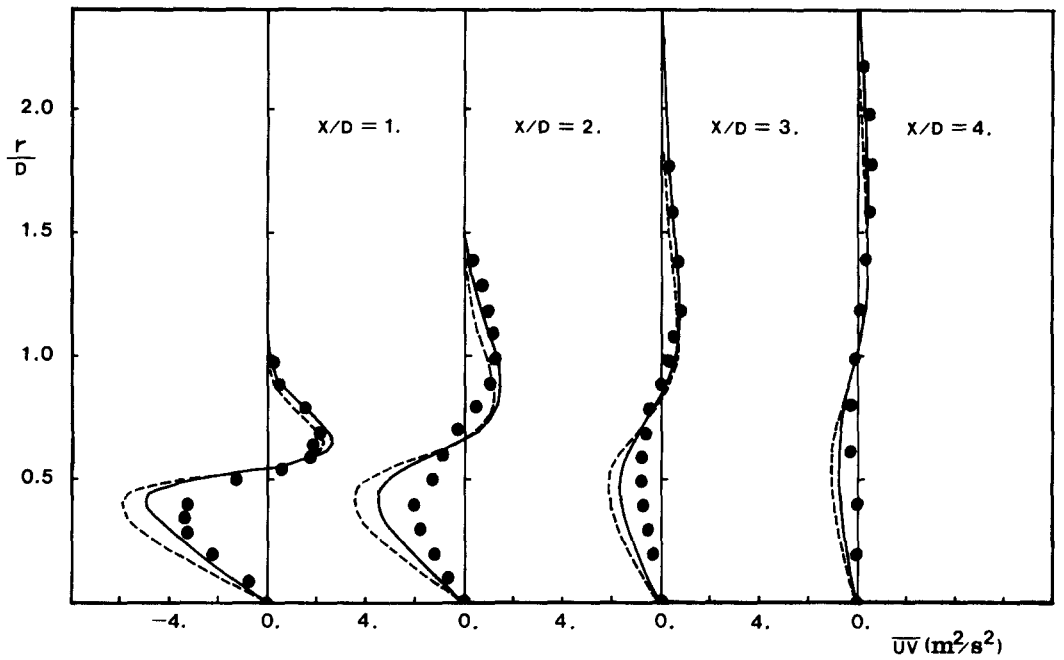

Figure 4 Distributions of shear stress, $\overline{uv}$ (symbols as in Figure 2)

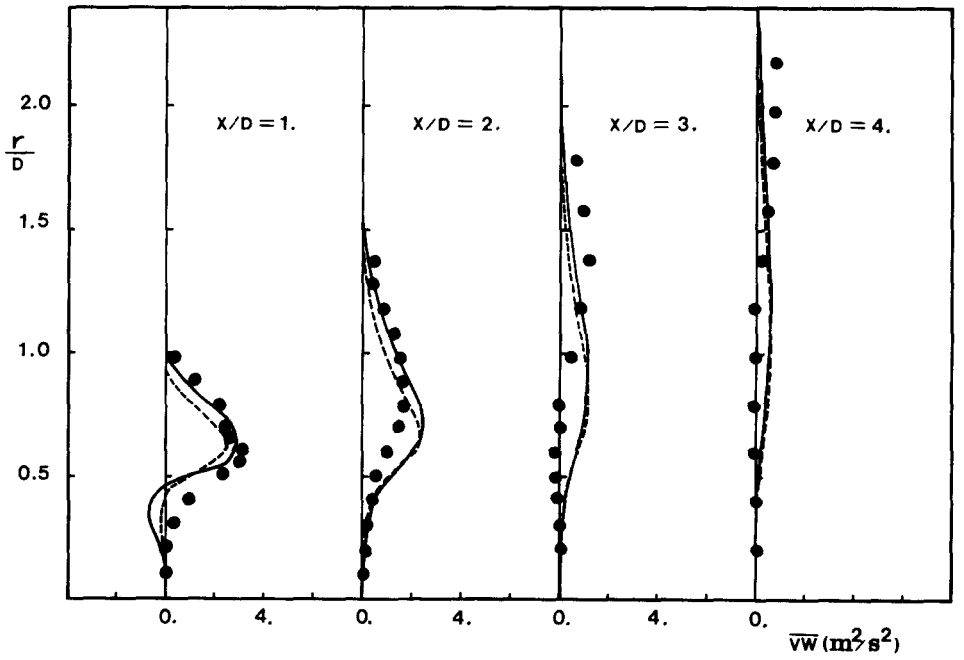

Figure 5 Distributions of shear stress, $\overline{vw}$ (symbols as in Figure 2)

stress model and the standard k-ε model for predictions of mean velocities U, V, and W in the flow field of a swirling jet with recirculation. The results are compared with the experiment of Sislian and Cusworth.[6] In the experiment, the swirl number was 0.79, and the Reynolds number, based on the average velocity at the nozzle exit, was 1.16×10^4. During the initial effort of the present study, it was found that the skew-upwind difference scheme[27] gives results no better than the hybrid central/upwind difference scheme in this particular case of the swirling jet, and that the inlet distribution of ε has a great influence on the computational results of the radial velocity profiles, as in Ref. 11.

Axial and tangential velocity profiles are represented in Figure 2 and Figure 3, respectively. The algebraic stress model is shown to yield more accurate predictions than the k-ε model on both velocity components. It is found that the standard k-ε model generally overestimates the maximum velocities and underestimates the jet spreading.

Figure 4 and Figure 5 show the distributions of shear stresses $\overline{uv}$ and $\overline{vw}$, respectively. In both figures, the algebraic stress model also gives better results compared to those of the standard k-ε model. However, in Figure 4, both computations underestimate the negative peak values of $\overline{uv}$. The computed locations of zero $\overline{uv}$ almost coincide with the measured locations of maximum axial velocity. As concluded by Sislian and Cusworth,[6] the experimental data show that the radial

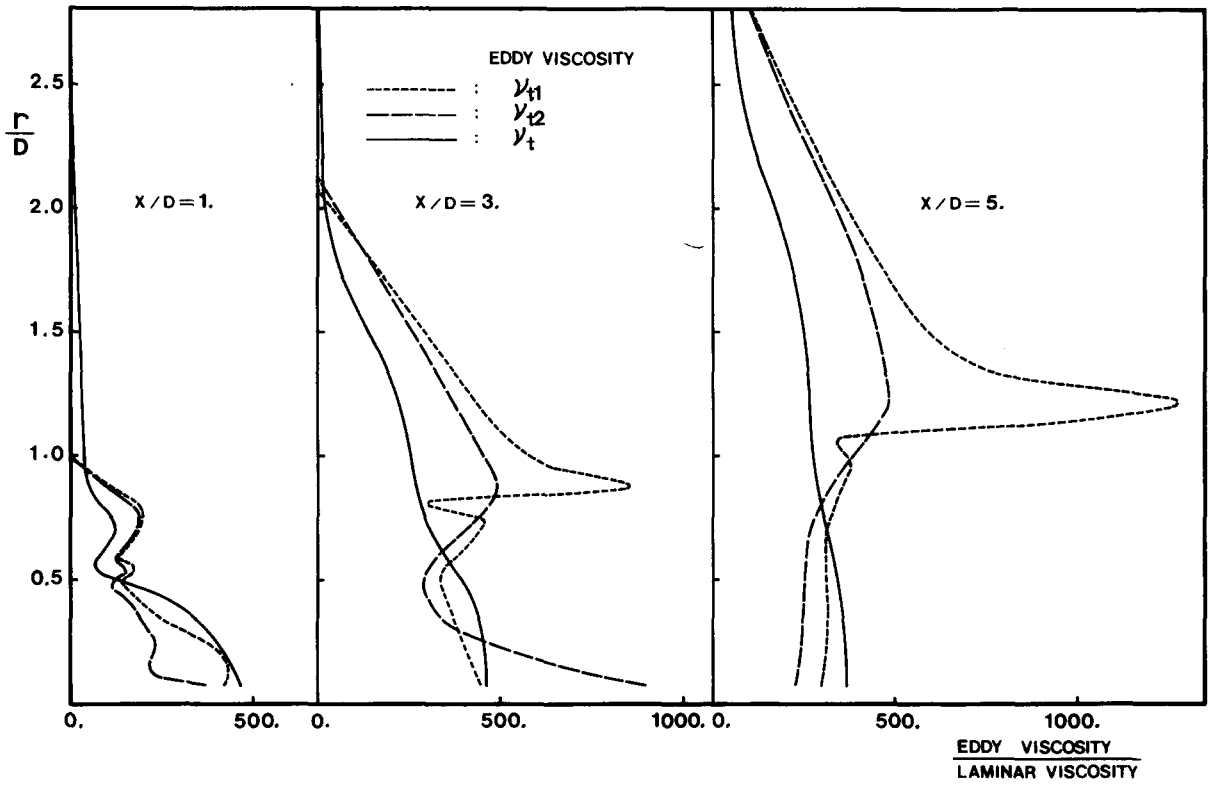

Figure 6 Distributions of eddy viscosities

positions of zero $\overline{uv}$ and zero $\partial U/\partial r$ almost coincide at all sections where the measurements are given, and that radial positions of minima and maxima of these quantities also coincide at all sections. The same is true for measured $\overline{vw}$ and $r\,\partial(W/r)/\partial r$ up to the section $x/D=2$. Further downstream the coincidence of these quantities deteriorates. Therefore, such a strong dependence of these shear stresses on the local strain rates of mean flow justifies the use of anisotropic eddy viscosities in the present algebraic stress model. However, due to the breakdown of the dependence of measured $\overline{vw}$ on $r\partial(W/r)/\partial r$ in the downstream of $x/D=2.$, the locations of computed maximum $\overline{vw}$ do not coincide with those of the measured ones in this region, as shown in Figure 5.

The anisotropies of directional eddy viscosities are shown in Figure 6, where the eddy viscosities defined by Equations 19 and 20 are compared with the eddy viscosity of the standard k-ε model. The largest difference between the computed eddy viscosities ν_{t_1} and ν_{t_2} occurs at the radial distance very close to the line of maximum mean velocity. In the downstream of the recirculation zone where the jet shows slender swirling shear layer behavior, the anisotropic eddy viscosities of the algebraic stress model are smaller than the isotropic eddy viscosity of the k-ε model in the stable region near the axis where the mean angular momentum increases with radius. The converse is shown in the unstable region. This phenomenon suggests that the algebraic stress model accounts for the effect of swirl, which is to diminish turbulent transport in stable flow and to augment it in unstable flow.

Conclusions

An algebraic stress model for the computation of axisymmetric swirling flows which accounts for the effect of swirl was derived. The equations for turbulent stresses were obtained by simplifying the Reynolds stress equations. The algebraic stress model was shown to predict the swirling jet flow with recirculation with an accuracy sufficient for practical purposes, and therefore it is concluded that the swirl effect can be simulated realistically.

References

1 Pratte, B. D. and Keffer, J. F. The swirling turbulent jet. *J. Fluid Engng., Trans. ASME*, 1972, **94**, 739–743

2 Ribeiro, M. M. and Whitelaw, J. H. Coaxial jets with and without swirl. *J. Fluid Mech.*, 1980, **96**, 769–795

3 Morse, A. P. Axisymmetric free shear flows with and without swirl. Ph.D. thesis, University of London, 1980

4 Dixon, T. F., Truelove, J. S., and Wall, T. F. Aerodynamic studies on swirled coaxial jets from nozzles with divergent quarls. *J. Fluid Engng.,Trans. ASME*, 1983, **105**, 197–203

5 Komori, S. and Ueda, H. Turbulent flow structure in the near field of a swirling round free jet. *Physics Fluids*, 1985, **28**, 2075–2082

6 Sislian, J. P. and Cusworth, R. A. Measurements of mean velocity and turbulent intensities in a free isothermal swirling jet. *AIAA J.*, 1986, **24**, 303–309

7 Morse, A. P. Flows with swirl. Proc. 1980–81 AFOSR-HTTM Stanford Conf. on Complex Turbulent Flows I, Stanford, Stanford University, 1982, 317–325

8 Bradshaw, P. The analogy between streamline curvature and buoyancy in turbulent shear flow. *J. Fluid Mech.*, 1969, **36**, 177–191

9 Launder, B. E., Priddin, C. H., and Sharma, B. I. The calculation of turbulent boundary layers on spinning and curved surfaces. *J. Fluid Engng., Trans. ASME*, 1977, **99**, 231–239

10 Rodi, W. Influence of buoyancy and rotation on equation for the turbulent length scale. Proc. 2nd Symp. on Turbulent Shear Flows, London, Imperial College, 1979, 10.37–10.42

11 Leschziner, M. A. and Rodi, W. Computation of strongly swirling axisymmetric free jets. *AIAA J.*, 1984, **22**, 1742–1747

12 Chen, C. P. Calculation of confined swirling jets. *Comm. Appl. Numer. Meths.*, 1986, **2**, 333–338

13 Launder, B. E. and Morse, A. Numerical prediction of axisymmetric free shear flows with a Reynolds stress closure. In: *Turbulent shear flows I*, Springer, Berlin, 1979, 279–294
14 Higuchi, H. and Rubesin, M. W. Behavior of a turbulent boundary layer subjected to sudden transverse strain. *AIAA J.*, 1979, **17**, 931–941
15 Ettestad, D. and Lumley, J. L. Parameterization of turbulent transport in swirling flows: theoretical considerations. In: *Turbulent shear flows 4*, Springer, Berlin, 1985, 87–101
16 Gibson, M. M. and Younis, B. A. Calculation of swirling jets with a Reynolds stress closure. *Physics Fluids*, 1986, **29**, 38–48
17 Gibson, M. M. and Younis, B. A. Calculation of boundary layers with sudden transverse strain. *J. Fluid Engng., Trans. ASME*, 1986, **108**, 470–475
18 Rodi, W. and Scheuerer, G. Calculation of curved shear layers with two-equation turbulence models. *Physics Fluids*, 1983, **26**(6), 1422–1436
19 Koosinlin, M. L. and Lockwood, F. C. The prediction of axisymmetric turbulent swirling boundary layers. *AIAA J.*, 1974, **12**, 547–554
20 Hah, C. Calculation of various diffuser flows with inlet swirl and inlet distortion effects. *AIAA J.*, 1983, **21**, 1127–1133
21 Kim, K. Y. and Chung, M. K. New eddy viscosity model for computation of swirling turbulent flows. *AIAA J.*, 1987, **25**, 1020–1022
22 Launder, B. E., Reece, G. J., and Rodi, W. Progress in the development of a Reynolds stress turbulent closure. *J. Fluid Mech.*, 1975, **68**, 537–566
23 Rodi, W. A new algebraic relation for calculating the Reynolds stresses. *Z. Angew. Math. Mech.*, 1976, **56**, 210–221
24 Gibson, M. M. An algebraic stress and heat-flux model for turbulent shear flow with streamline curvature. *Int. J. Heat Mass Transfer*, 1978, **21**, 1609–1617
25 Scott, G. J. and Rask, D. R. Turbulent viscosities for swirling flow in a stationary annulus. *J. Fluid Engng., Trans. ASME*, 1973, **95**, 557–566
26 Lilley, D. G. and Rhode, D. L. A computer code for swirling turbulent axisymmetric recirculating flows in practical isothermal combustor geometries. NASA CR-3442, 1982
27 Raithby, G. D. Skew-upwind differencing schemes for problems involving fluid flow. *Comp. Meth. Appl. Mech. Engng.*, 1976, **9**, 153–164